1   **Title:**   **Anti-inflammatory activity and molecular mechanism of Oolong tea**

2   **theasinensin**

3

4   **Authors:**   Ayami Hisanaga[a]**,** Hisako Ishida[b], Kozue Sakao[a, b], Takayuki Sogo[a],

5   Takuma Kumamoto[a], Fumio Hashimoto[a, b], De-Xing Hou [a, b,¶]

6   **Affiliations:**   [a]United Graduate School of Agricultural Science, [b]Faculty of Agriculture,

7   Kagoshima University, Kagoshima 890-0065, Japan.

8

9   **Running Title: Anti-inflammatory effects of Oolong tea theasinensin**

10

11

12   **[¶]Corresponding author:** Professor De-Xing Hou, Faculty of Agriculture, Kagoshima University,

13   Korimoto 1-21-24, Kagoshima, 890-0065, Japan.

14   E-mail: hou@chem.agri.kagoshima-u.ac.jp (D.-X Hou)**,** Fax/Tel: +81 99 285 8649

15

16   *Abbreviations:*

17   COX-2, cyclooxygenase-2; ERK, extracellular signal-regulated kinase; FBS, fetal

18   bovine serum; IL-12, interleukin-12; iNOS, inducible nitric oxide synthase; *i.p.*,

19   intraperitoneally; LPS, lipopolysaccharide; MAPK, mitogen-activated protein kinase;

20   MCP-1, monocyte chemotactic protein-1; MEK, MAPK/ERK kinase; NF-κB, nuclear

21   factor-kappa B; NO, nitric oxide; PGE_2 , prostaglandin E_2; *s.c.*, subcutaneously; TNF-α,

22   tumor necrosis factor alpha; TSA, Theasinensin A.

23

24

25

26 Abstract

27 Oolong tea theasinensins are a group of tea polyphenols different with green tea

28 catechins and black tea theaflavins, and are considered to bioactive compounds in

29 oolong tea. Based on the properties of theasinensin and the information of inflammation

30 processes, we investigated the anti-inflammatory activity and molecular mechanisms of

31 theasinensin A (TSA) in both cell and animal models in the present study. In the cell

32 model, TSA reduced the levels of proinflammatory mediators including inducible nitric

33 oxide synthase (iNOS), nitric oxide (NO), interleukin-12 (IL-12) (p70), tumor necrosis

34 factor alpha (TNF-α), and monocyte chemotactic protein-1 (MCP-1) induced by

35 lipopolysaccharide (LPS). Cellular signaling analysis revealed that TSA downregulated

36 MAPK/ERK kinase (MEK)-extracellular signal-regulated kinase (ERK) signaling.

37 Pull-down assay and affinity data revealed that TSA might directly bind to MEK-ERK

38 for the inhibitory action. In the animal model, TSA suppressed the production of IL-12

39 (p70), TNF-α, and MCP-1 and attenuated mouse paw edema induced by LPS.

40

41 **Keywords:** Theasinensin A; MEK-ERK; pro-inflammatory cytokines, mouse paw

42 edema; anti-inflammation

43

44

45

46

47

48

49

1. Introduction

Tea polyphenols can be divided into three kinds according to the fermentation during tea processing.[1, 2] One is green tea without fermentation, and catechins such (-) epigallocatechin-gallate (EGCG) are the representative primary polyphenols. Second is black tea with completed fermentation. The representative secondary polyphenols are theaflavins. Both catechins and theaflavins have been extensively studies on chemopreventive efficacy in multiple organs, and have been considered to be potent compounds for chemoprevention.[3, 4] Third is Oolong tea with partial fermentation, which is consumed heavily in Asian countries. From Oolong tea, we have isolated a number of theasinensins (namely, A, B, C, D, and E),[1, 2] which are major secondary polyphenols formed during the partial fermentation processes, and possess antioxidative effects against lipid peroxidation.[5] In our previous study, we have found that theasinensins revealed the potential to inhibit cyclooxygenase-2 (COX-2) expression in lipopolysaccharide (LPS)-activated mouse macrophage-like cells (RAW264.7) with a relationship of structure-activity.[6] Among five kinds of theasinesins, theasinensin A (TSA) and D (TSD) revealed strongest inhibition on both COX-2 expression and prostaglandin (PG) E_2 production, suggesting that the galloyl moiety play an important role on the inhibitory action of theasinensins because TSA and TSD bearing two galloyl moieties showed strongest inhibitory effect while TSC and TSE bearing no galloyl moiety failed to show the inhibitory effect in the same conditions.[6] Therefore, we chose TSA as a target to investigate the inhibitory effects on pro-inflammatory cytokines and underlying mechanisms.

During inflammatory disease, the primary cells of chronic inflammation are macrophages that produce excess amounts of mediators such as nitric oxide (NO) and

74 pro-inflammatory cytokines such as interleukin-12 (IL-12) (p70), tumor necrosis factor

75 alpha (TNF-α), and monocyte chemotactic protein-1 (MCP-1).[7, 8] In inflammatory site,

76 NO is generated from *L*-arginine by inducible nitric oxide synthase (iNOS).[9] NO

77 overproduction leads to various harmful responses including apoptosis and necrosis.[10]

78 TNF-α is involved in many different cellular processes by producing numerous

79 cytokines and acute phase proteins to cause many pathophysiologic processes.[11, 12]

80 IL-12(p70) is a proinflammatory mediator providing an important link between the

81 activation of innate immune cells and the induction of an effective adaptive immune

82 response.[13] MCP-1 is a pro-inflammatory chemokine capable of promoting monocyte

83 recruitment into an inflammatory or pathological site to produce more pro-inflammatory

84 mediators.[14] Therefore, these pro-inflammatory cytokines play pivotal roles in

85 consequences of inflammation.[15]

86   Although the cellular signaling pathways regulating the inflammation are very

87 complicated, mitogen-activated protein kinase (MAPK) and nuclear factor-kappa B

88 (NF-κB) pathways have been suggested at least to key pathways in the expression of

89 inflammatory mediators.[7, 8] MAPK can stimulate the production of inflammatory

90 mediators such as COX-2, iNOS and cytokines in bacterial LPS-activated

91 macrophages.[16, 17, 18] In our previous study, we demonstrated that TSA and

92 prodelphinidin could suppress COX-2 expression by downregulating MAPK.[6, 19]

93 Moreover, recent several lines of studies have showed that polyphenolic compounds can

94 directly bind to MAPK protein to attenuate the kinase signaling. For example,

95 myricetin,[20] quercetin,[21] procyanidin B2[22] could directly bind to MAPK/ERK kinase

96 (MEK) to attenuate MEK phosphorylation and downstream signaling. These data

97 suggest that MEK is potential primary target for some bioactive polyphenolic

98 compounds.

99   Based on the bioactive properties of theasinensins and the information of

100   inflammation processes, we investigated the anti-inflammatory activity of TSA and

101   underlying mechanisms using both cell and animal models in the present study. First of

102   all, we used RAW264.7 cells, which can be stimulated with LPS to mimic a status of

103   infection and inflammation, to investigate the inhibition and molecular mechanisms of

104   TSA on the production of pre-inflammatory mediators. Finally, we confirmed the

105   anti-inflammatory effects *in vivo,* using a mouse paw edema model.

106

107   **2.   Results**

108   **2.1 The inhibitory effects of TSA on the production of inflammatory factors**

109   To investigate the effect of TSA on the production of inflammatory factors such as

110   NO/iNOS, IL-12 (p70), TNF-α, and MCP-1, RAW264.7 cells were treated with 25-100

111   μM of TSA for 30 min, respectively, before exposure to 40 ng/ml LPS for 12 h. As

112   shown in Fig. 2A, LPS-induced NO production was significantly suppressed by TSA.

113   And TSA also inhibited LPS-induced iNOS expression in a dose-dependent manner (Fig.

114   2B).

115   Many cytokines have been reported to act as inflammatory factors. To clarify whether

116   TSA influences these cytokine productions, we examined the levels of 23 kinds of

117   cytokines in the supernatant of such treatment cells by Bio-Plex Pro Mouse Cytokine

118   23-Plex Panel kit (Bio-Rad Laboratories). LPS treatment for 12 h enhanced more than

119   five-fold level of G-CSF, TNF-α, RANTES, IL-6, MCP-1, GM-CSF, more than

120   two-fold level of IL-12 (p70), KC, MIP-1β, IL-1α, IL-10, IL-9; and less than two-fold

121   in IL-13, IL-1β, IL-4, IL-17, IL-3, IFN-γ, IL-12 (p40), Eotaxin, IL-5, MIP-1α, IL-2,

122   comparing with that of the cells without LPS treatment (Hou *et al*., unpublished data).

123   Pretreatment with TSA at the indicated concentrations decreased significantly the level

124 of IL-12 (p70), TNF-α, and MCP-1 (Fig. 3) in the concentrations of 25-50 μM, but TSA

125 did not affect significantly other 20 kinds of cytokines (data not shown).

126

127 **2.2   Modulation of TSA on MEK-ERK signaling**

128 MAPK signaling is one of the important cell signaling pathways that regulates

129 cytokines and pro-inflammatory mediators such as IL-12 (p70), TNF-α, MCP-1 and

130 iNOS during inflammatory response. Thus, we investigated the effects of TSA on the

131 LPS-induced phosphorylation of MEK-extracellular signal-regulated kinase (ERK) in

132 RAW264.7 cells. The cells were treated with 50 μM of TSA for 30 min, respectively,

133 before exposed to 40 ng/ml LPS for 30 min. As shown in Fig. 4, treatment with 40

134 ng/ml LPS for 30 min caused phosphorylation of ERK1/2. Pretreatment with 50 μM

135 TSA for 30 min suppressed markedly their phosphorylation. To confirm this, we further

136 examined the effects on the phosphorylation of MEK1, an upstream kinase of ERK1/2.

137 The same inhibitory effect was also observed in the phosphorylation of MEK1. These

138 data indicate that the downregulation of MEK-ERK is at least involved in the inhibition

139 of LPS-induced inflammation by TSA.

140

141 **2.3   Binding ability of TSA to MEK and ERK *ex vivo* and *in vitro***

142 In previous studies, MEK-ERK have been suggested as a potential targets for TSA to

143 inhibit the inflammatory signaling.[6, 20-22] Thus, we investigated whether the TSA bind to

144 MEK, using bead-bound pull-down assay which has been validated as effective

145 screening tool in our previous study.[23] TSA was coupled with CNBr-sepharose 4B beads,

146 and then incubated with protein lysate extracted from RAW264.7 cells *ex vivo*. MEK or

147 ERK was detected by Western blotting with antibody after washing out. As shown in

148 Fig. 5A, MEK1 and ERK1/2 were detected in the Sepharose 4B beads coupled with

149   TSA (0.8, 0.9-fold), but not in Sepharose 4B beads alone. To further confirm the binding

150   specificity, we used recombinant MEK1 and ERK2 (active) for *in vitro* pull-down assay,

151   higher amount of MEK1 and ERK2 bound were detected in Sepharose 4B beads, but

152   not in Sepharose 4B beads alone (Fig. 5B). These data suggest that TSA could bind to

153   MEK and ERK directly.

154

155   **2.4   Affinity of TSA to MEK1, and ERK2 proteins**

156   In order to know the binding affinity of TSA to MEK1 and ERK2, we used QCM assay

157   to investigate the disassociation constant (K_d) of TSA to these protein kinases. As shown

158   in Fig. 6, TSA showed K_d values of 6.48 μM for MEK1 (Fig. 6A), and 5.52 μM for

159   ERK2 (Fig. 6B), respectively. Small K_d value means low disassociation with higher

160   binding affinity, thus, ERK2 might be more potential target for TSA because ERK2

161   showed the lowest K_d value.

162

163   **2.5   Inhibition of LPS-induced paw edema in mice**

164   To further confirm the anti-inflammatory effects of TSA *in vivo,* we used the model of

165   mouse paw edema induced by LPS. The mice were divided into three groups: control,

166   LPS, LPS plus TSA. Each group had three mice, respectively. TSA was injected

167   intraperitoneally (*i.p.*) (30 mg/kg body weight) for 4 days before LPS treatment. LPS

168   was injected *i.p.* and subcutaneously (*s.c.*) (1 mg/kg body weight), and the paw

169   thickness was measured using digital caliper before and every hour after LPS treatment

170   until 6 h (Fig. 7A). The results showed that LPS treatment increased the paw thickness

171   from 2.63 to 3.39 mm at 1 h, and 2.94 mm after 6 h. Pretreatment with TSA for 4 days

172   reduced the LPS-induced paw thickness to 3.10 mm at 1 h, and 2.81 mm after 6 h. TSA

173   decreased the edema by 64.4 %, compared with LPS alone after 6 h. As a control,

174   treatment with PBS concluding 2 % DMSO did not show any effect on paw edema (Fig.

175   7B). Simultaneously, we checked the levels of three serum cytokines, which were

176   induced by LPS in RAW264.7 cells (Fig. 3), by Bio-Plex Mouse cytokine assay. As

177   shown in Fig. 7C, pretreatment with TSA decreased the levels of LPS-induced serum

178   IL-12 (p70), TNF-α, and MCP-1. These data confirmed *in vivo* the anti-inflammatory

179   effect of TSA that attenuated the production of LPS-induced inflammatory mediators to

180   inhibit mouse paw edema.

181

182   **3. Discussion**

183   In the present study, we investigated the anti-inflammatory properties of an oolong tea

184   polyphenol, TSA, in both cell and animal models. In the cell model, we demonstrated

185   that TSA suppressed the productions of NO/iNOS, IL-12 (p70), TNF-α, and MCP-1 by

186   targeting MEK-ERK molecules at least. In the animal model, we observed that TSA

187   suppressed mouse paw edema with attenuation in the level of serum IL-12 (p70),

188   TNF-α, and MCP-1 (Fig. 7). Thus, our data demonstrated the anti-inflammatory effects

189   and underlying mechanisms of TSA *in vitro* and *in vivo*.

190   Accordingly, polyphenols can interact by hydrogen bonding with almost all the proteins

191   giving an association which decrease them solubility.[24] This can be referred as

192   "non-specific binding".[25] Recently, several lines of studies have demonstrated that

193   polyphenols revealed "specific binding" capacity with some proteins including some

194   kinases beyond "non-specific binding".[25, 26, 27] Our previous studies have showed that

195   TSA could suppress the expression of inflammatory mediators such as COX-2 and

196   PGE$_2$ by attenuating cellular signaling including MAPK and NF-κB pathways, and

197   suggested that MEK-ERK may be direct targets for TSA.[6] In the present study, we

198   investigated the potential that TSA binds to MEK-ERK, using bead-bound pull-down

199 assay which has been validated as effective screening tool in our previous study.[23] MEK

200 and ERK were detected in the Sepharose 4B beads coupled with TSA and cellular lysate,

201 but not in Sepharose 4B beads alone (Fig. 5A). The direct binding was further

202 confirmed with purified recombinant protein of MEK or ERK (Fig. 5B). Moreover, in

203 vitro affinity analysis by QCM showed that TSA had binding affinity to MEK1 and

204 ERK2 proteins (Fig.6) although the affinity appears weaker that other pharmaceutical

205 specific inhibitors. These data supported that TSA might target MEK and ERK

206 molecules by directly binding. Our data with the results of other groups also revealed

207 that the specificity and binding affinity of polyphenols are accordingly less than that of

208 pharmaceutical kinase inhibitors.[20-22] According to the properties of pharmaceutical

209 kinase inhibitors and dietary polyphenols, we can consider that small-molecule

210 pharmaceuticals are designed for defined target specificity, dietary polyphenols affect a

211 large number of cellular targets with varied affinities that, combined, result in their

212 recognized health benefits.

213   A limitation of the in vitro studies is that they do not take into account the

214 absorption and bioavailability of TSA. *In vivo* studies have showed that TSA was

215 absorbable polyphenols through intestinal tight-junction with intact form into rat blood,

216 [28] and exerted anti-hyperglycemic effect when TSA is administered to KK-Ay mice for

217 6 weeks. [29] Pharmacokinetic analyses revealed that TSA was rapidly absorbed to rat

218 blood within 1 h. The C_{max} and $AUC_{0-6\,h}$ values of TSA were 9.3 ± 1.8 nM and $16.7 \pm$

219 1.0 nmol h L^{-1}, respectively, after the oral administration of TSA (100 mg/kg) to

220 Sprague-Dawley rats.[28] However, in *in vitro* cell model (rat skeletal muscle cells, L6

221 myoblasts), 25-50 μM of TSA was required to exert the anti-hyperglycemic effect

222 through the CaMKK/AMPK signaling pathway.[30] According to the information, we

223 used the same range of concentration of TSA for *in vitro* cell model (RAW264.7).

224   Moreover, due to the intact absorption of TSA[28] and the limitation of purified TSA

225   amount, we chose 30 mg TSA / kg mouse weight for *in vivo* model by *i.p.* injection,

226   which is available for this case to get the intact TSA as oral administration. The reasons

227   for TSA concentration difference between *in vitro* and *in vivo* models are not fully

228   understood. One of considerable reasons is that the analysis of conjugates or metabolites

229   of TSA were not performed in previous *in vivo* absorption investigation [28] although the

230   methylation and sulfation of theasinensins have been reported to be present.[31]

231   Accumulated data have revealed that the conjugates of some dietary polyphenols are

232   indeed bioactive forms *in vivo* although the concentration is very low.[32]   However, the

233   conjugates of dietary polyphenols in *in vitro* cell model remain unclear although they

234   are considered as very low concentration. That is one possible important reason why

235   higher concentration of dietary polyphenols is required in *in vitro* cell model to exert the

236   bioactivities while a relatively lower concentration *in vivo* shows the bioactivities. In

237   future study, we like to clarify TSA conjugates *in vivo*, and use its conjugates at

238   appropriate concentrations for *in vitro* cell model to clarify the biological response what

239   might occur *in vivo*.

240

241   **4. Materials and methods**

242   **4.1 Reagents and cell culture**

243   TSA (Fig. 1) was isolated from oolong tea in the former report,[2] and purified by HPLC

244   with 99% purity. The final concentration of DMSO with TSA was 0.2% in cell culture.

245   LPS (*Escherichia coli* Serotype 055:B5) was from Sigma (St. Louis, MO, USA). The

246   antibodies against iNOS, MEK1 and α-tubulin were from Santa Cruz Biotechnology Inc.

247   (Santa Cruz, CA, USA). All of antibodies used were from Cell Signaling Technology

248   (Beverly, MA, USA). CNBr-activated Sepharose 4B was from GE Healthcare.

249   Recombinant MEK1 and ERK2 were from Abcam. RAW264.7 cells were purchased

250   from the American Type Culture Collection (Manassas, VA, USA) and cultured in

251   Dulbecco's modified Eagle's medium (DMEM) containing 10% fetal bovine serum

252   (FBS), 4 mM *L*-glutamine.

253

254   **4.2   Measurement of NO production**

255   NO production was measured with Griess method.[33] In brief, RAW264.7 macrophage

256   cells (3×10^5 cells/well) were seeded into each well of 48-well plates. After incubation

257   for 21 h, cells were starved by being cultured in serum-free medium for another 2.5 h to

258   eliminate FBS influence. The cells were then treated with or without TSA for 30 min

259   before expose to 40 ng/ml LPS for 12 h. The NO production in the culture medium was

260   determined by measuring absorbance at 550 nm.

261

262   **4.3   Cytokine determination by the multi-plex technology**

263   The method has been described in our previous report.[34] In brief, RAW264.7 cells ($1.2 \times$

264   10^5 cells/well) were seeded into each well of 12-well plates. After incubation for 21 h,

265   cells were starved by being cultured in serum-free medium for another 2.5 h to

266   eliminate FBS influence. The cells were then treated with or without TSA for 30 min

267   before expose to 40 ng/ml LPS for 12 h. The culture medium was used to assay the

268   cytokine production with Bio-Plex Pro Mouse Cytokine 23-Plex Panel kit (Bio-Rad

269   Laboratories) for 23 cytokines including IL-1α, IL-1β, IL-2, IL-3, IL-4, IL-5, IL-6, IL-9,

270   IL-10, IL-12(p40), IL-12(p70), IL-13, IL-17, Eotaxin, G-CSF, GM-CSF, IFN-γ, KC,

271   MCP-1, MIP-1α, MIP-1β, RANTES, and TNF-α in a Bio-Plex machine (Bio-Plex 200

272   System, Bio-Rad). The assay was performed according to the manufacturer's

273   instructions (Bio-Rad Laboratories) and analyzed with the Bio-Plex manager software

274 (version 5.0). The blood serum collected from heart blood was used for the

275 measurement of 23 mouse cytokines with the same method as described above.

276

277 **4.4 Western blotting**

278 Western blotting assay was performed as described previously.[33] Briefly, RAW264.7

279 cells (1×10^6 cells/dish) were cultured in 6-cm dishes for 21 h, cells were starved by

280 being cultured in serum-free medium for another 2.5 h to eliminate influence of FBS.

281 The cells were then treated with or without TSA for 30 min before expose to 40 ng/ml

282 LPS for the indicated times. The cells were lysed in a lysate buffer, and boiled for 5 min.

283 Approximate 20-40 μg of proteins were run on 10% SDS-PAGE and then transferred to

284 PVDF membrane (GE Healthcare, UK). The blotted membrane was incubated with

285 specific primary antibody for overnight at 4 °C and further incubated for 1 h with

286 HRP-conjugated secondary antibody. Bound antibodies were detected by ECL agent and

287 further quantified by Lumi Vision Imager software (TAITEC Co., Japan).

288

289 **4.5 *Ex vivo* and *in vitro* pull-down assay**

290 *Ex vivo* and *in vitro* pull-down assay was performed as described in our previous

291 paper.[23] Briefly, TSA (5 μM) were coupled to CNBr-activated Sepharose 4B beads (25

292 mg) in a coupling buffer [0.5 M NaCl, 0.1 M NaHCO$_3$ (pH 8.3) and 25 % DMSO] for

293 overnight at 4 °C according to the manufacturer's instructions. The mixture was washed

294 with 5 volumes of coupling buffer and then resuspended with 5 volumes of 0.1 M

295 Tris-HCl buffer (pH 8.0) with 2 h rotation at room temperature (RT) to block any

296 remaining active groups. After washing three cycles with acetate buffer [0.1 M acetic

297 acid (pH 4.0) and 0.5 M NaCl] followed by with wash buffer [0.1 M Tris-HCl (pH 8.0)

298 and 0.5 M NaCl]. The RAW264.7 cell lysate (500 μg), recombinant MEK1 (100 ng) or

299   ERK2 (100 ng) was then incubated overnight at 4 °C with Sepharose 4B beads,

300   TSA-conjugated Sepharose 4B beads (100 μl, 50% slurry) in a reaction buffer [50 mM

301   Tris-HCl (pH 8.5), 5 mM EDTA, 150 mM NaCl, 1mM DTT, 0.01% Nonidet P-40, 2

302   μg/ml BSA, 0.02 mM PMSF and 1 μg protease inhibitor cocktail]. The beads were

303   washed 5 times with 50 mM Tris-HCl (pH 7.5) containing 5 mM EDTA, 200 mM NaCl,

304   1 mM DTT, 0.02% Nonidet P-40 and 0.02 mM PMSF. The proteins bound to the beads

305   were analyzed by Western blotting with MEK1 or ERK antibody.

306

307   **4.6   Quartz-crystal microbalance (QCM)**

308   Recombinant MEK1, or ERK2 protein (100 ng) was immobilized into a QCM electrode

309   plate for 1 h at RT. After washing with binding buffer [50 mM Tris-HCl (pH 8.0), 150

310   mM NaCl, 1 mM EDTA and 2 μg/ml BSA], electrode plate was dipped into 8 ml

311   binding buffer at 25 °C. TSA was injected stepwise into the analysis chamber (0.1–25.6

312   μM). The binding affinity was indicated by frequency changes of QCM, and binding

313   disassociation constant (K_d) was calculated by AFFINIX Q User Software (AQUA,

314   Initium, Japan)

315

316   **4.7 In vivo paw edema model**

317   The animal experiments were conducted in accordance with the guidelines of the

318   Animal Care and Use Committee of Kagoshima University. Male ICR mice (4 weeks

319   old) from Japan SLC Inc were group-house under controlled light (12 h light/day) and

320   temperature (25 °C). All the animals had free access to water and feed in a home cage.

321   The mice were randomly divided into three groups: control, LPS, LPS plus TSA. TSA

322   was dissolved in PBS containing 2% DMSO and administered to the mice by *i.p.*

323   injection at 30 mg /kg body weight for 4 days before LPS treatment. LPS were injected

324   *i.p.* and *s.c.* to paw with 100 μl of 0.3 mg/ml (1 mg/kg body weight) and 10 μl of 3

325   mg/ml (1 mg/kg body weight) respectively. Paw thickness was measured using caliper

326   (model 19975, Shinwa Rules Co. Ltd) before and every hour after LPS treatment until 6

327   h. After 6 h, mice were sacrificed and blood serum was collected for cytokines assay.

328

329   **4.8   Statistical analysis**

330   The difference between treated and control cells were analyzed by analysis of variance

331   tests. Means with differently lettered superscripts differ significantly at the probability

332   of $p < 0.05$.

336

337   **References**

338   1   G. Nonaka, O. Kawahara, I. Nishioka, Tannins and related compounds. XV. A new

339   class of dimeric flavan-3-ol gallates, theasinensins A and B, and proanthocyanidin

340   gallates from green tea leaf. (1). *Chem. Pharm. Bull.* 1983, **31,** 3906-3914.

341   2   F. Hashimoto, G. Nonaka, I. Nishioka, Tannins and related compounds. LXIX.

342   Isolation and structure elucidation of B, B'-linked bisflavanoids, theasinensins D-G

343   and oolongtheanin from Oolong tea. (2). *Chem. Pharm. Bull.* 1988, **36,** 1676-1684.

344   3   N. Khan, F. Afaq, M. Saleem, N. Ahmad, et al., Targeting multiple signaling

345   pathways by green tea polyphenol (-)-epigallocatechin-3- gallate. *Cancer Res.*

346   2006, **66,** 2500-2505.

347   4   C.S. Yang, J.D. Lambert, Z. Hou, J. Ju, et al., Molecular targets for the cancer

348   preventive activity of tea polyphenols. *Molecu. Carcinogenesis*, 2006, **45,** 431-435.

349   5   F. Hashimoto, M. Ono, C. Masuoka, Y. Ito, et al., Evaluation of the anti-oxidative

350   effect (*in vitro*) of tea polyphenols. *Biosci. Biotechnol. Biochem.* 2003, **67,**

351   396-401.

352   6   D.-X. Hou, S. Masuzaki, S. Tanigawa, F. Hashimoto, et al., Oolong tea theasinensins

353   attenuate cyclooxygenase-2 expression in lipopolysaccharide (LPS)-activated

354   mouse macrophages: structure-activity relationship and molecular mechanisms. *J.*

355   *Agric Food Chem.* 2010, **58,** 12735-12743.

356   7   D.L. Laskin, J.D. Laskin, Role of macrophages and inflammatory mediators in

357   chemically induced toxicity, *Toxicology*, 2001, **160,** 111-118.

358   8   S.H. Lee, S.Y. Lee, D.J. Son, H. Lee, et al, Inhibitory effect of

359   2′-hydroxycinnamaldehyde on nitric oxide production through inhibition of NF-κB

360   activation in RAW 264.7 cells, *Biochem. Pharmacol.* 2005, **69,** 791-799.

361   9   C. Nathan, Q.W. Xie, Nitric oxide synthases: Roles, tolls, and controls, *Cell*, 1994,

362   **78,** 915-918.

363   10 H. Nagai, H. Kumamoto, M. Fukuda, T. Takahashi, Inducible nitric oxide synthase

364   and apoptosis-related factors in the synovial tissues of temporomandibular joints

365   with internal derangement and osteoarthritis, *J. Oral Maxillofac. Surg.* 2003, **61,**

366   801-807.

367   11 Z.G. Liu, Molecular mechanism of TNF signaling and beyond, *Cell Res.* 2005, **15,**

368   24-27.

369   12 G. Sethi, B. Sung, B.B. Aggarwal, TNF: A master switch for inflammation to

370   cancer, *Front Biosci.* 2008, **13,** 5094-5107.

371   13 M. Rossol, H. Heine, U. Meusch, D. Quandt, et al., LPS-induced cytokine

372   production in human monocytes and macrophages. *Crit. Rev. Immunol.* 2011, **31,**

373   379–446.

374   14   H.Y. Park, N.D. Kim, G.Y. Kim, H.J. Hwang, et al., Inhibitory effects of diallyl

375   disulfide on the production of inflammatory mediators and cytokines in

376   lipopolysaccharide-activated BV2 microglia, *Toxicol. Appl. Pharmacol.* 2012, **262,**

377   177-184.

378   15   J.J. Hadad, Cytokines and related receptor-mediated signaling pathways,

379   *Biochem. Biophys. Res. Commun.* 2002, **297,** 700-713.

380   16   C. Chen, Y.H. Chen, W.W. Lin, Involvement of p38 mitogen-activated protein

381   kinase in lipopolysaccharide-induced iNOS and COX-2 expression in J774

382   macrophages, *Immunology,* 1999, **97,** 124-129.

383   17   L. Chang, M. Karin, Mammalian MAP kinase signalling cascades, *Nature,* 2001,

384   **410,** 37-40.

385   18   S.J. Ajizian, B.K. English, E.A. Meals, Specific Inhibitors of p38 and Extracellular

386   Signal-Regulated Kinase Mitogen-Activated Protein Kinase Pathways Block

387   Inducible Nitric Oxide Synthase and Tumor Necrosis Factor Accumulation in

388   Murine Macrophages Stimulated with Lipopolysaccharide and Interferon-γ, *J.*

389   *Infect. Dis.* 1999, **179,** 939-944.

390   19   D.-X. Hou, D. Luo, S. Tanigawa, F. Hashimoto, et al., Prodelphinidin B-4

391   3′-*O*-gallate, a tea polyphenol, is involved in the inhibition of COX-2 and iNOS via

392   the downregulation of TAK1-NF-κB pathway, *Biochem. Pharmacol.* 2007, **74,**

393   742-751.

394   20   K.W. Lee, N.J. Kang, E.A. Rogozin, H.G. Kim, et al., Myricetin is a novel natural

395   inhibitor of neoplastic cell transformation and MEK1, *Carcinogenesis,* 2007, **28,**

396   1918–1927.

397   21   K.W. Lee, N.J. Kang, Y.S. Heo, E.A. Rogozin, et al., Raf and MEK protein

398   kinases are direct molecular targets for the chemopreventive effect of quercetin, a

399   major flavonols in red wine. *Cancer Res*, 2008, **68,** 946–955.

400 22 N.J. Kang, K.W. Lee, D.E. Lee, E.A. Rogozin, et al., Cocoa procyanidins suppress

401   transformation by inhibiting mitogen-activated protein kinase kinase, *J. Biol. Chem.*

402   2008, **283,** 20664–20673.

403 23 T. Kumamoto, M. Fujii, D.-X. Hou, Akt is a direct target for myricetin to inhibit

404   cell transformation. *Mol. Cell Biochem.* 2009, **332,** 33-41.

405 24 P. Bandyopadhyay, A.K. Ghosh, C. Ghosh, Recent developments on

406   polyphenol–protein interactions: effects on tea and coffee taste, antioxidant

407   properties and the digestive system. *Food Funct.*, 2012, **3**, 592-605.

408 25 C.G. Fraga, M. Galleano, S.V. Verstraeten, P.I. Oteiza, Basic biochemical

409   mechanisms behind the health benefits of polyphenols. *Mol Aspects Med.* 2010, **31,**

410   435-445.

411 26 D.-X Hou, T. Kumamoto, Flavonoids as protein kinase inhibitors for cancer

412   chemoprevention: direct binding and molecular modeling. *Antioxid Redox Signal.*

413   2010 **13,** 691-719.

414 27 D. Arango, K. Morohashi, A. Yilmaz, K. Kuramochi, et al., Molecular basis for the

415   action of a dietary flavonoid revealed by the comprehensive identification of

416   apigenin human targets. *Proc Natl Acad Sci USA.* 2013, **110,** 2153-2162.

417 28 J. Qiu, Y. Kitamura, Y. Miyata, S. Tamaru, et al., Transepithelial transport of

418   theasinensins through Caco-2 cell monolayers and their absorption in

419   Sprague-Dawley rats after oral administration. *J Agric Food Chem.* 2012, **60,**

420   8036-8043.

421 29 Y. Miyata, S. Tamaru, T. Tanaka, K. Tamaya, et al., Theaflavins and theasinensin

422   A derived from fermented tea have antihyperglycemic and hypotriacylglycemic

423 effects in KK-A^y mice and Sprague-Dawley rats. *J Agric Food Chem.* 2013, **61,**

424 9366–9372.

425 30 J. Qiu, K. Maekawa, Y. Kitamura, Y. Miyata, et al., Stimulation of glucose uptake

426 by theasinensins through the AMP-activated protein kinase pathway in rat skeletal

427 muscle cells. *Biochem Pharmacol.* 2014, **87,** 344-351.

428 31 A.P. Neilson, B.J. Song, T.N. Sapper, J.A. Bomser, et al., Tea catechin

429 auto-oxidation dimers are accumulated and retained by Caco-2 human intestinal

430 cells. *Nutr. Res.* 2010, **30,** 327-340.

431 32 P.A. Kroon, M.N. Clifford, A. Crozier, A.J. Day, et al., How should we assess the

432 effects of exposure to dietary polyphenols in vitro? <u>*Am J Clin Nutr.*</u> 2004, **80,**

433 15-21.

434 33 T. Uto, M. Fujii, D.-X. Hou, 6-(Methylsulfinyl)hexyl isothiocyanate suppresses

435 inducible nitric oxide synthase expression through the inhibition of Janus kinase

436 2-mediated JNK pathway in lipopolysaccharide-activated murine macrophages,

437 *Biochem. Pharmacol.* 2005, **70,** 1211-1221.

438 34 S. You, E. Nakanishi, H. Kuwata, J. Chen, et al., Inhibitory effects and molecular

439 mechanisms of garlic organosulfur compounds on the production of inflammatory

440 mediators. *Mol. Nutr. Food Res.* 2013, **57,** 2049-2060.

441

442

443

444

445

446

447

448   **Figure Legends:**

449

450   **Fig. 1.** The chemical structure of theasinensin A (TSA)

451

452   **Fig.2.** Influence of TSA on the production of NO (A) and iNOS (B). RAW264.7 cells

453   were precultured for 21 h, and starved in serum-free medium for 2.5 h. The cells were

454   then treated with the indicated concentrations of TSA for 30 min, and then exposed to

455   40 ng/ml LPS for 12 h. iNOS protein and α-tubulin were detected by Western blotting

456   with their antibodies, respectively. The induction fold was calculated as the intensity of

457   the treatment relative to that of control by densitometry. The blots shown are the

458   examples of three separate experiments. Means with differently lettered superscripts

459   differ significantly at the probability of $p < 0.05$.

460

461   **Fig. 3.** Influence of TSA on the production of IL-12 (p70) (A), TNF-α (B), and

462   MCP-1(C). The culture and treatment of RAW264.7 cells were performed as described

463   in Fig.1. The amount of cytokines in medium was measured, using the multi-plex

464   technology as described in Section 4.3. Each value represents the mean $\pm$ S.D. of

465   triplicate cultures. Means with differently lettered superscripts differ significantly at the

466   probability of $p < 0.05$.

467

468   **Fig. 4.** TSA suppress the phosphorylation of ERK1/2 and MEK1/2. RAW264.7 cells

469   were pre-cultured for 21 h, and starved in serum-free medium for 2.5 h. After treatment

470   with the indicated concentration of TSA for 30 min, the cells were further exposed to 40

471   ng/ml LPS for 30 min. The phosphorylated protein kinases and α-tubulin were detected

472   with their antibodies, respectively. The induction fold of the phosphorylated kinase was

473   calculated as the intensity of the treatment relative to that of control normalized to

474   α-tubulin by densitometry. The blots shown are the examples of three separate

475   experiments.

476

477   **Fig. 5.** Binding abilities of TSA to MEK-ERK. (A) *Ex vivo* pull-down assay. Whole cell

478   lysate (input control, *lane 1*), lysate precipitation with Sepharose 4B beads (negative

479   control, *lane 2*) and Sepharose 4B-TSA-coupled beads (*lane 3*) were applied to

480   SDS-PAGE and then detected with MEK1 and ERK1/2 antibodies. (B) *In vitro*

481   pull-down assay. Active MEK1 or ERK2 (input control, *lane 1*), active MEK1 or ERK2

482   precipitation with Sepharose 4B beads (negative control, *lane 2*) and Sepharose

483   4B-TSA-coupled beads (*lane 3*) were applied to SDS-PAGE and then detected with

484   MEK1 and ERK1/2 antibodies. The binding efficiency of MEK-ERK to TSA was

485   presented as the ratio of input control, respectively.

486

487   **Fig. 6.** Affinity of TSA for MEK1, and ERK2 proteins. His-tagged MEK1 or ERK2

488   protein was immobilized into a QCM electrode plate for 1 h at room temperature and

489   then immersed in the analysis chamber after washing. TSA was injected and recorded

490   by frequency changes of QCM. The K_d value was calculated with the AQUA software.

491

492   **Fig. 7.** TSA suppresses paw edema in mice. The mice were divided into three groups:

493   control, LPS, LPS plus TSA. Each group had three mice, respectively. TSA was injected

494   *i.p.* (30 mg/kg body weight) for 4 days, and LPS was then injected *i.p.* and *s.c.* at paw (1

495   mg/kg body weight). The mouse paw thickness was measured using digital caliper

496   before and every hour after LPS treatment until 6 h (A). The change of paw edema

497   thickness was shown in (B). Means with differently lettered superscripts differ

498   significantly at the probability of $p < 0.05$. The change in level of serum IL-12 (p70),

499   TNF-α and MCP-1 is shown in (C). The blood serums were obtained from the mice that

500   were treated with or without LPS for 6 h by collection of heart blood. The amount of

501   cytokines in serum was measured as described in Section 4.3. Each value represents the

502   mean $\pm$ S.D. of three mice. Means with differently lettered superscripts differ

503   significantly at the probability of $p < 0.05$.
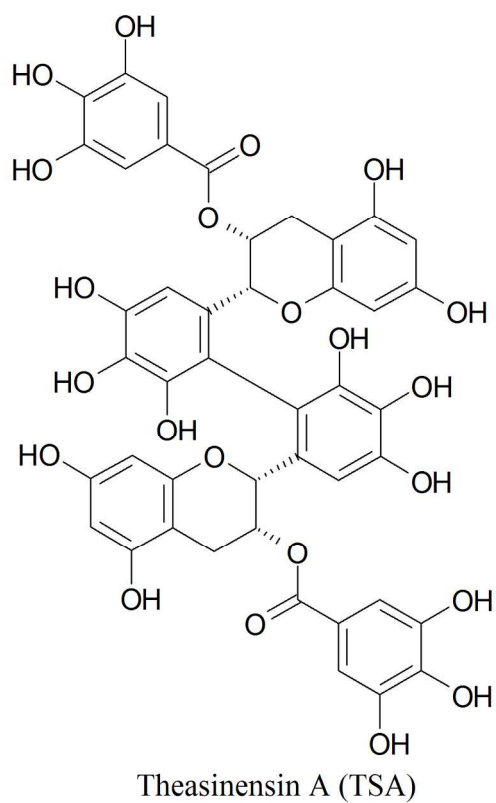
Theasinensin A (TSA)

Fig.1 Hisanaga et al.

Fig. 1. The chemical structure of theasinensin A (TSA)
164x219mm (300 x 300 DPI)
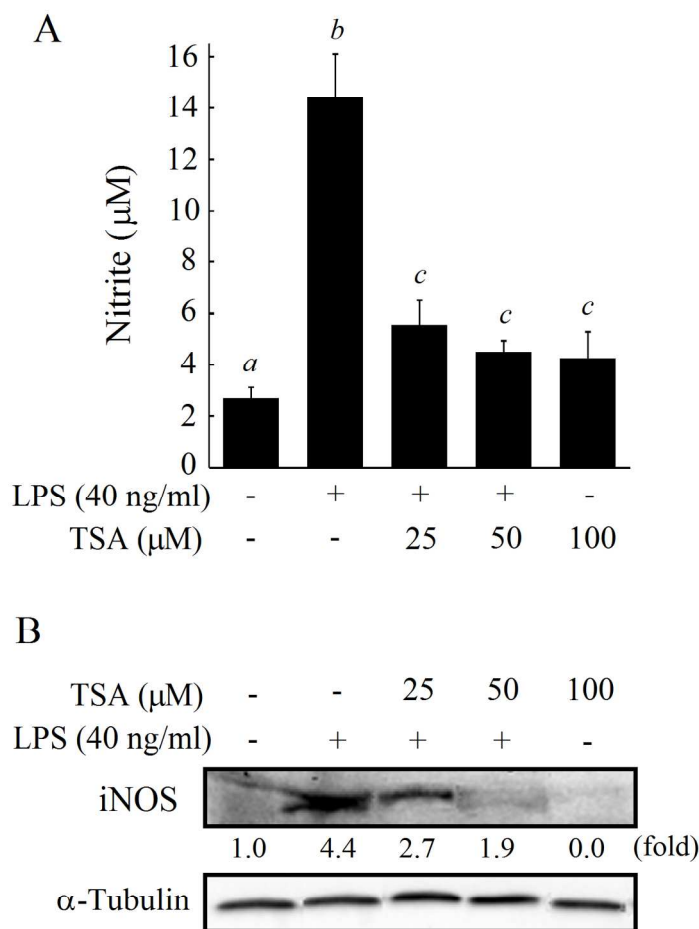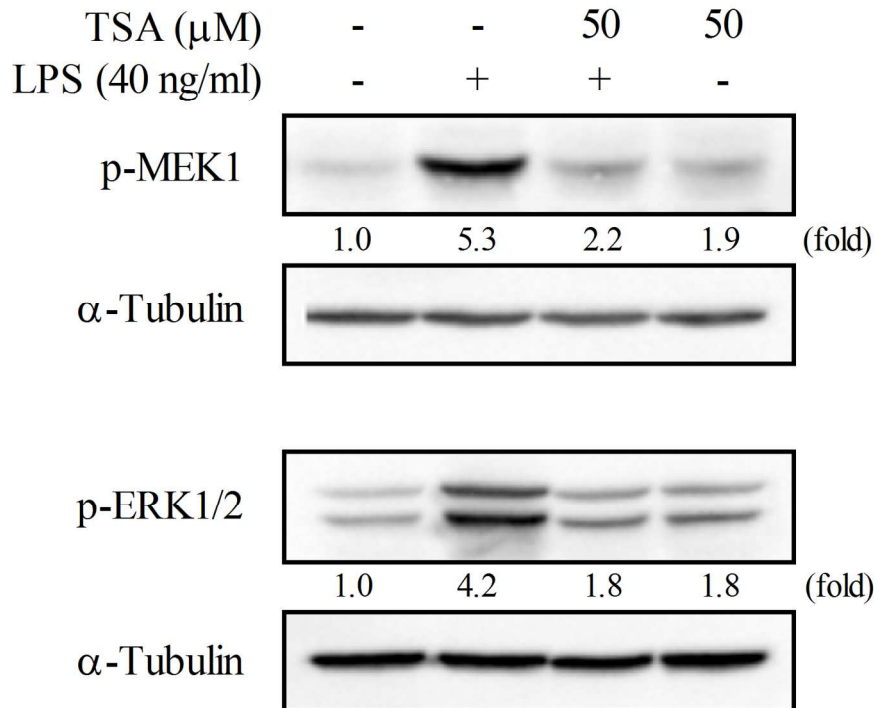
Fig.2 Hisanaga et al.

Fig.2. Influence of TSA on the production of NO (A) and iNOS (B). RAW264.7 cells were precultured for 21 h, and starved in serum-free medium for 2.5 h. The cells were then treated with the indicated concentrations of TSA for 30 min, and then exposed to 40 ng/ml LPS for 12 h. iNOS protein and α-tubulin were detected by Western blotting with their antibodies, respectively. The induction fold was calculated as the intensity of the treatment relative to that of control by densitometry. The blots shown are the examples of three separate experiments. Means with differently lettered superscripts differ significantly at the probability of $p < 0.05$. 123x193mm (300 x 300 DPI)
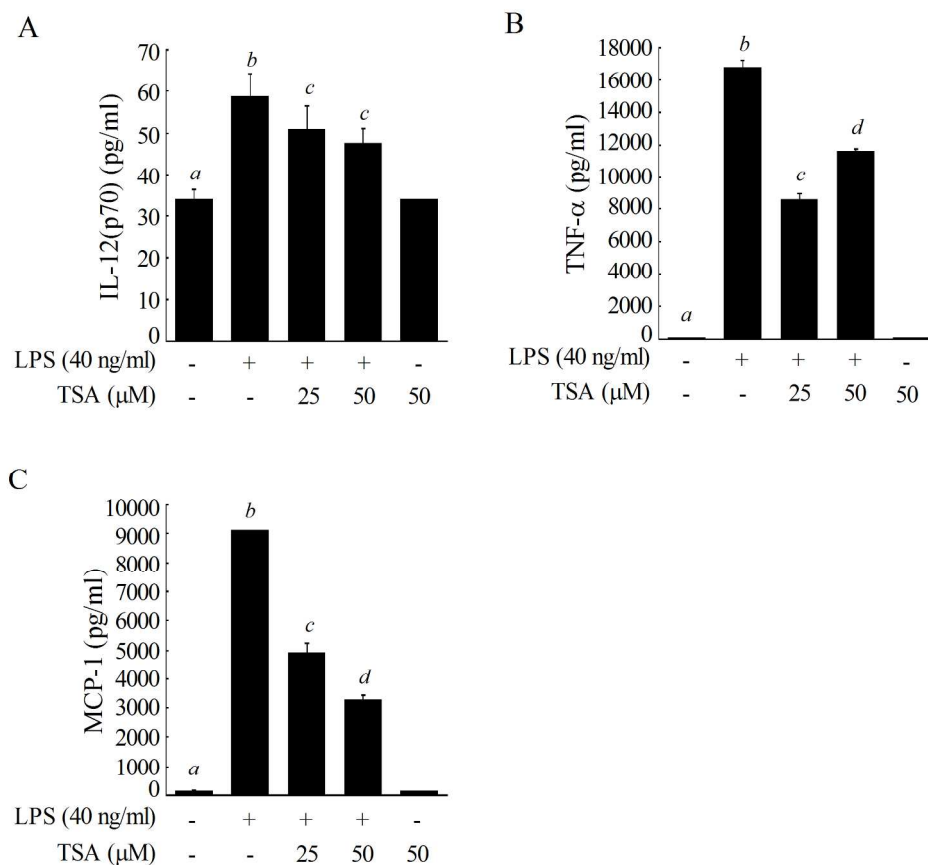
Fig.3 Hisanaga et al.

Fig. 3. Influence of TSA on the production of IL-12 (p70) (A), TNF-α (B), and MCP-1(C). The culture and treatment of RAW264.7 cells were performed as described in Fig.1. The amount of cytokines in medium was measured, using the multi-plex technology as described in Section 4.3. Each value represents the mean ± S.D. of triplicate cultures. Means with differently lettered superscripts differ significantly at the probability of $p < 0.05$.
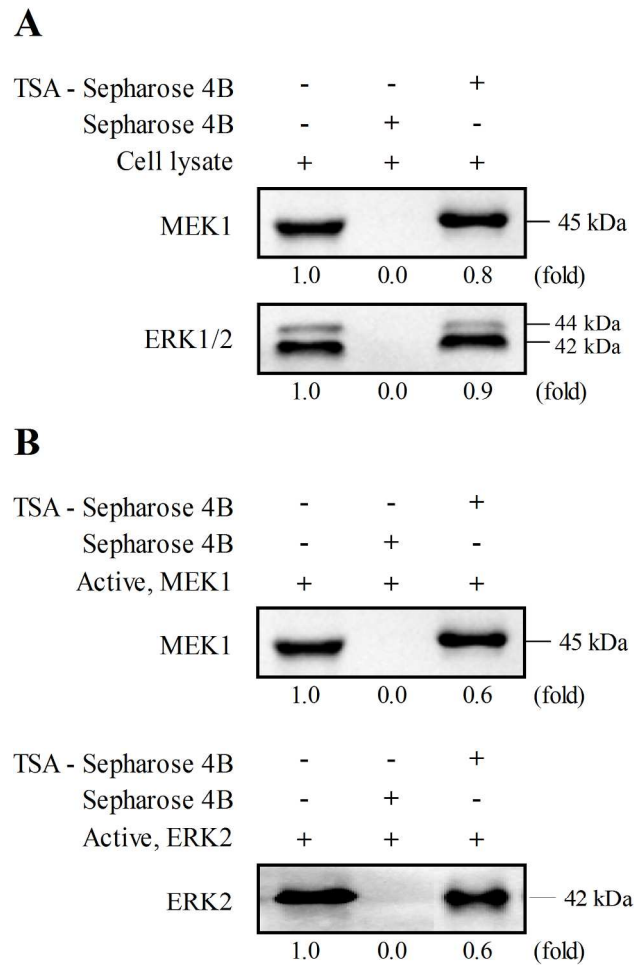215x212mm (300 x 300 DPI)

Fig. 4 Hisanaga et al.

Fig. 4. TSA suppress the phosphorylation of ERK1/2 and MEK1/2. RAW264.7 cells were pre-cultured for 21 h, and starved in serum-free medium for 2.5 h. After treatment with the indicated concentration of TSA for 30 min, the cells were further exposed to 40 ng/ml LPS for 30 min. The phosphorylated protein kinases and α-tubulin were detected with their antibodies, respectively. The induction fold of the phosphorylated kinase was calculated as the intensity of the treatment relative to that of control normalized to α-tubulin by densitometry. The blots shown are the examples of three separate experiments.
154x156mm (300 x 300 DPI)

A

TSA - Sepharose 4B	-	-	+
Sepharose 4B	-	+	-
Cell lysate	+	+	+

MEK1 — 45 kDa

1.0	0.0	0.8	(fold)

ERK1/2 — 44 kDa / 42 kDa

1.0	0.0	0.9	(fold)

B

TSA - Sepharose 4B	-	-	+
Sepharose 4B	-	+	-
Active, MEK1	+	+	+

MEK1 — 45 kDa

1.0	0.0	0.6	(fold)

TSA - Sepharose 4B	-	-	+
Sepharose 4B	-	+	-
Active, ERK2	+	+	+

ERK2 — 42 kDa

1.0	0.0	0.6	(fold)

Fig.5 Hisanaga et al.

Fig. 5. Binding abilities of TSA to MEK-ERK. (A) Ex vivo pull-down assay. Whole cell lysate (input control, lane 1), lysate precipitation with Sepharose 4B beads (negative control, lane 2) and Sepharose 4B-TSA-coupled beads (lane 3) were applied to SDS-PAGE and then detected with MEK1 and ERK1/2 antibodies. (B) In vitro pull-down assay. Active MEK1 or ERK2 (input control, lane 1), active MEK1 or ERK2 precipitation with Sepharose 4B beads (negative control, lane 2) and Sepharose 4B-TSA-coupled beads (lane 3) were applied to SDS-PAGE and then detected with MEK1 and ERK1/2 antibodies. The binding efficiency of MEK-ERK to TSA was presented as the ratio of input control, respectively.
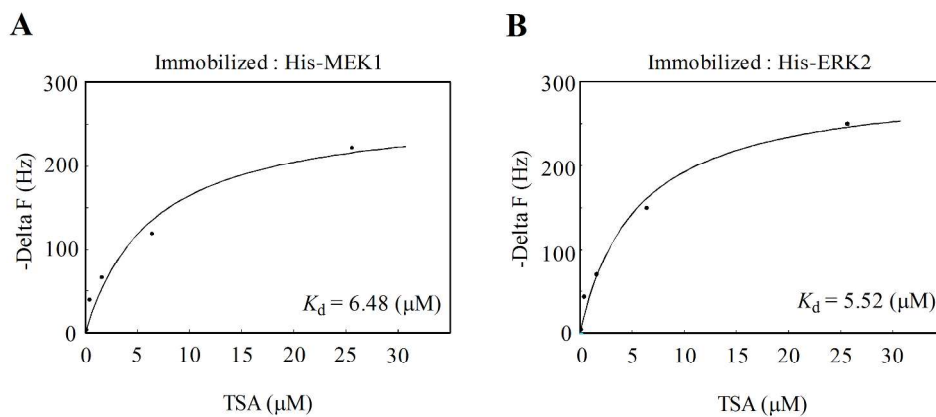149x252mm (300 x 300 DPI)

A

Immobilized : His-MEK1

$K_d = 6.48$ (μM)

B

Immobilized : His-ERK2

$K_d = 5.52$ (μM)

Fig.6 Hisanaga et al.

Fig. 6. Affinity of TSA for MEK1, and ERK2 proteins. His-tagged MEK1 or ERK2 protein was immobilized into a QCM electrode plate for 1 h at room temperature and then immersed in the analysis chamber after washing. TSA was injected and recorded by frequency changes of QCM. The Kd value was calculated with the AQUA software.
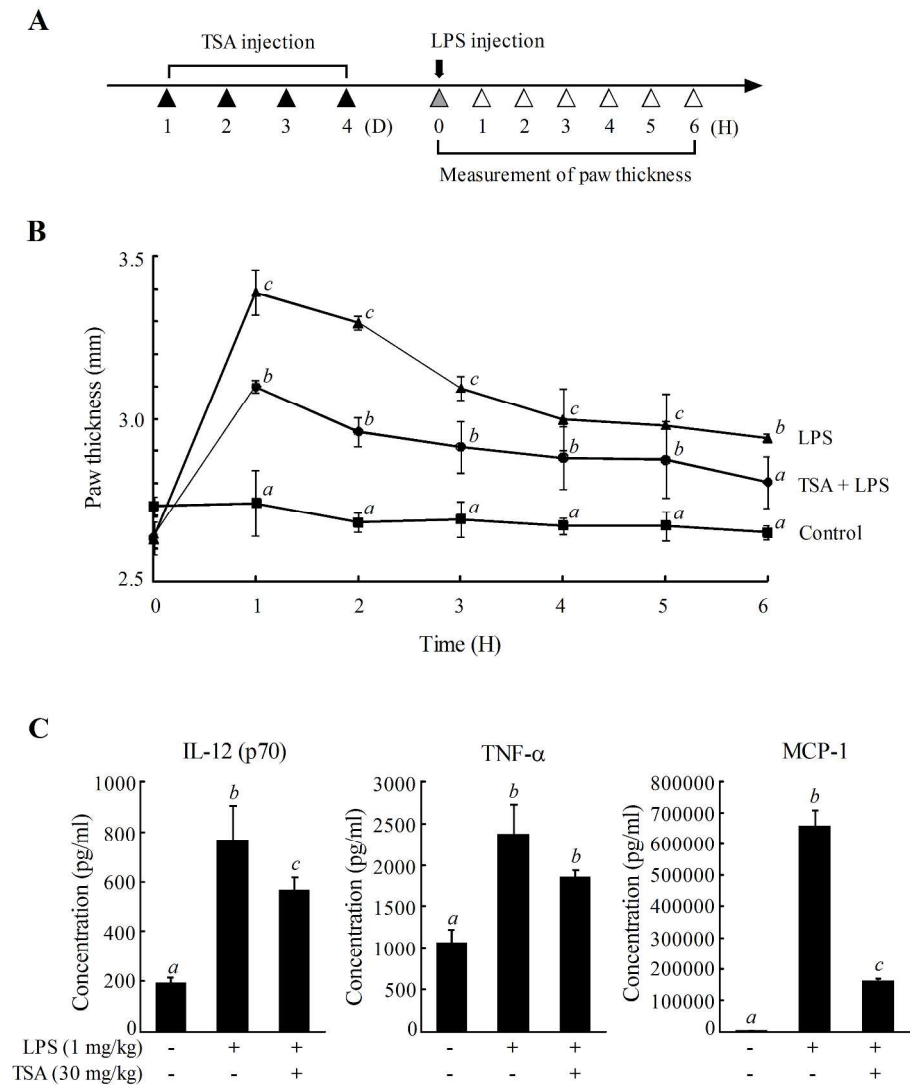258x153mm (300 x 300 DPI)

A

TSA injection

LPS injection

1   2   3   4   (D)   0   1   2   3   4   5   6   (H)

Measurement of paw thickness

B

C

IL-12 (p70)   TNF-α   MCP-1

LPS (1 mg/kg)   -   +   +
TSA (30 mg/kg)   -   -   +

Fig. 7 Hisanaga et al.

Fig. 7. TSA suppresses paw edema in mice. The mice were divided into three groups: control, LPS, LPS plus TSA. Each group had three mice, respectively. TSA was injected i.p. (30 mg/kg body weight) for 4 days, and LPS was then injected i.p. and s.c. at paw (1 mg/kg body weight). The mouse paw thickness was measured using digital caliper before and every hour after LPS treatment until 6 h (A). The change of paw edema thickness was shown in (B). Means with differently lettered superscripts differ significantly at the probability of $p < 0.05$. The change in level of serum IL-12 (p70), TNF-α and MCP-1 is shown in (C). The blood serums were obtained from the mice that were treated with or without LPS for 6 h by collection of heart blood. The amount of cytokines in serum was measured as described in Section 4.3. Each value represents the mean ± S.D. of three mice. Means with differently lettered superscripts differ significantly at the probability of $p < 0.05$.

257x337mm (300 x 300 DPI)